analytical chemistry

pubs.acs.org/ac Article

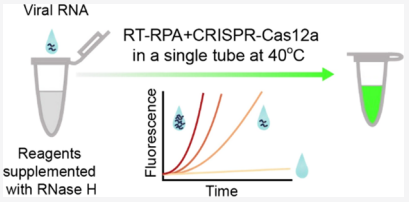
Integrating Reverse Transcription Recombinase Polymerase Amplification with CRISPR Technology for the One-Tube Assay of RNA

Wei Feng,[▽] Hanyong Peng,[▽] Jingyang Xu, Yanming Liu, Kanti Pabbaraju, Graham Tipples, Michael A. Joyce, Holly A. Saffran, D. Lorne Tyrrell, Shawn Babiuk, Hongquan Zhang,* and X. Chris Le*

Cite This: *Anal. Chem.* 2021, 93, 12808−12816 Read Online

ACCESS | Metrics & More | Article Recommendations | Supporting Information

ABSTRACT: CRISPR-Cas systems integrated with nucleic acid amplification techniques improve both analytical specificity and sensitivity. We describe here issues and solutions for the successful integration of reverse transcription (RT), recombinase polymerase amplification (RPA), and CRISPR-Cas12a nuclease reactions into a single tube under an isothermal condition (40 °C). Specific detection of a few copies of a viral DNA sequence was achieved in less than 20 min. However, the sensitivity was orders of magnitude lower for the detection of viral RNA due to the slow initiation of RPA when the complementary DNA (cDNA) template remained hybridized to RNA. During the delay of RPA, the crRNA-Cas12a ribonucleoprotein (RNP) gradually lost its activity in the RPA solution, and nonspecific amplification reactions consumed the RPA reagents. We overcame these problems by taking advantage of the endoribonuclease function of RNase H to remove RNA from the RNA-cDNA hybrids and free the cDNA as template for the RPA reaction. As a consequence, we significantly enhanced the overall reaction rate of an integrated assay using RT-RPA and CRISPR-Cas12a for the detection of RNA. We showed successful detection of 200 or more copies of the S gene sequence of SARS-CoV-2 RNA within 5−30 min. We applied our one-tube assay to 46 upper respiratory swab samples for COVID-19 diagnosis, and the results from both fluorescence intensity measurements and end-point visualization were consistent with those of RT-qPCR analysis. The strategy and technique improve the sensitivity and speed of RT-RPA and CRISPR-Cas12a assays, potentially useful for both semi-quantitative and point-of-care analyses of RNA molecules.



INTRODUCTION

CRISPR technology has significantly advanced genome editing as well as molecular detection.[1−5] CRISPR-associated (Cas) proteins can target different genes of interest with a corresponding guide RNA designed to be complementary to the target nucleic acids.[6] This programmable RNA-guided site-specific recognition is simpler than the mechanisms of previous genome editing tools because CRISPR-Cas eliminates the need to engineer individual proteins for targeting each site.[7] In the CRISPR-Cas reaction cascade, target recognition activates Cas systems to either operate on the target nucleic acids for gene editing or function as a *trans*-cleavage nuclease to cleave collaterally nucleic acid reporters for molecular detection.[1,4,8,9] CRISPR-based diagnostics modularly combines nucleic acid amplification techniques with the target-specific detection capability of CRISPR-Cas systems. Combining isothermal amplification with CRISPR-Cas is especially advantageous for potential point-of-care applications. Isothermal amplification, such as loop-mediated isothermal amplification (LAMP)[10] and recombinase polymerase amplification (RPA),[11] can exponentially amplify DNA rapidly to improve analytical sensitivity but is susceptible to nonspecific amplification, which weakens analytical specificity if target-specific detection probes are not used. Following isothermal exponential amplification, CRISPR-Cas systems specifically detect the amplicon of target molecules and thus improve analytical specificity.[5] Thus, methods of combining nucleic acid amplification with CRISPR-Cas have been successfully applied to the detection of pathogens, including SARS-CoV-2, the causative agent of the coronavirus disease of 2019 (COVID-19).[12−14]

Limited by the incompatibility of the reaction temperature and reagents, most isothermal assays used the CRISPR technology for detection in a separate post-amplification step.[8,13,15] However, opening tubes after exponential amplification risks contaminating the working environment with the DNA amplicons and causing false positives.[16] Therefore, it is desirable to complete both the amplification and detection in the same tube without opening the tube after the amplification step.

Received: August 12, 2021
Published: September 10, 2021



Downloaded via SHANGHAI NORMAL UNIV on March 23, 2022 at 07:38:38 (UTC).
See https://pubs.acs.org/sharingguidelines for options on how to legitimately share published articles.

ACS Publications

© 2021 The Authors. Published by American Chemical Society

https://doi.org/10.1021/acs.analchem.1c03456
Anal. Chem. 2021, 93, 12808−12816

RPA typically operates at a moderate temperature (e.g., 40 °C),[11] matching the optimal reaction temperatures of most Cas enzymes, such as Cas13a and Cas12a.[17] Cas12a recognizes double-stranded DNA (dsDNA) and is suitable for the direct detection of dsDNA amplicons. Cas13a recognizes RNA and requires an extra step of T7 transcription of DNA amplicons for detection. Although RPA and CRISPR-Cas systems have been integrated into single-tube assays,[8,18−26] most of these assays require the separate placement of RPA and CRISPR-Cas reagents to achieve sensitive detection (Supporting Information Table S1).[8,18,20−22] Ding et al.[23] recently developed a one-pot assay with the RT-RPA and CRISPR-Cas12a reactions taking place in the same solution. This assay used two crRNA-Cas12a ribonucleoproteins (RNPs), each activated by a displaced single-stranded region of the RPA amplicon, to generate fluorescence signals. However, the crRNA-Cas12a RNP is less specific for differentiating mismatches in single-stranded DNA (ssDNA) than in dsDNA.[8] Additionally, the use of the two RNPs requires the design of two crRNA sequences and increases the cost of the assay.

Previous studies also showed that the detection of RNA using RT-RPA and CRISPR-Cas is less sensitive than the detection of DNA,[13,24] the reason for which has not been well elucidated. We hypothesize that rapid initiation of RPA is critical for the success of a single-tube assay and that dynamic formation of RNA-cDNA hybrids delays the initiation of RPA. We report here our tests of the hypothesis, our understanding of the underlying problem, and an approach to overcoming the problem. Using the detection of SARS-CoV-2 RNA as an example, we reveal the importance of generating single-stranded cDNA for rapid RPA initiation in an integrated RT-RPA-CRISPR-Cas12a technique and demonstrate a single-tube assay for the rapid and semi-quantitative detection of a specific RNA target. To ensure the specificity of the assay, we design a crRNA to recognize the dsDNA of the RPA amplicons instead of recognizing the ssDNA. An additional benefit of using the crRNA targeting dsDNA is that the *trans*-cleavage activity of crRNA-Cas12a RNPs is higher for dsDNA than for ssDNA.[8] Thus, only one RNP is needed to generate readout signals for detection.

EXPERIMENTAL SECTION

SARS-CoV-2 Viral RNA. The original SARS-CoV-2 virus strain (SARS-CoV-2/CANADA/VIDO 01/2020) was obtained from the University of Saskatchewan, Canada. SARS-CoV-2 was produced from the infection of Vero-E6 cells at a multiplicity of infection (MOI) of 0.01 for 48 h followed by harvesting of the supernatant. The amount of SARS-CoV-2 RNA in the supernatant was measured by RT-quantitative PCR (RT-qPCR). RNA in 140 μL cell supernatants was isolated by using the QIAmp Viral RNA Mini kit (Qiagen) and reverse transcribed using the Superscript IV Vilo Master Mix (Invitrogen). The S gene and RdRp gene were quantified using a lab-developed RT-qPCR assay. A 2 μL aliquot of RNA extracts was mixed with the RT-qPCR master mix, which comprised 0.6 μL of 10 μM each primer, 0.5 μL of 10 μM probe, and 1× TaqPath 1-Step RT-qPCR Master Mix (ThermoFisher) to a final volume of 20 μL. The sequences of primers and probes and RT-PCR program are listed in Tables S2−S4.

RT-RPA and Cas12a Reactions in a Single Tube Assay. LbCas12a RNP containing 0.5 μM LbCas12a (NEB, M0653T) and 0.65 μM crRNA in 1× NEB buffer 2.1 was incubated at 37 °C for 0.5 h and kept on ice. Before each analysis, the RT mix for eight reactions was prepared by mixing 1 μL of 10× M-MuLV Buffer, 0.8 μL of RPA primer mix (50 μM each), 2 μL of 10 mM dNTP, 4 μL of 200 U/μL M-MuLV reverse transcriptase (NEB, M0253L), and 2 μL of 2 U/μL RNase H (ThermoFisher, 18021−014). The RPA mix was prepared by adding 52 μL of rehydration buffer, 0.8 μL of RPA primer mix (50 μM each), and 10 μL of 100 μM Cas12a reporter to two tubes of lyophilized RPA reagents (TwistAmp Basic Kit).

The single-tube assay was conducted in a MicroAmp Fast 8-Tube Strip (ThermoFisher, 4358293). To allow all reactions in the same batch to start at the same time with sufficient priming, 4 μL of sample and 1.1 μL of RT mix were added to the lid. Separate from this mixture, 1 μL of MgOAc (280 mM) was added to another location of the lid. LbCas12a RNP (1 μL) was added to the bottom of the tube, and the RPA mix (7 μL) was added to the wall of the tube. Then, the tubes were spun, and the reaction was mixed thoroughly (∼10 inversions) followed by another spin before real-time fluorescence monitoring (StepOnePlus Applied Biosystems). The single-tube RPA-Cas12a assay for DNA followed the same protocol except for omitting the RT mix but adding a total of 1.6 μL of RPA primer mix (50 μM each) into the RPA mix.

Analysis of Clinical Samples for the S Gene of SARS-CoV-2 RNA. We analyzed RNA extracts from 46 clinical specimens of Alberta, Canada residents, comprising 21 SARS-CoV-2 positive specimens and 25 SARS-CoV-2 negative specimens confirmed with an RT-qPCR assay.[27] RNA from each of the 46 respiratory nasopharyngeal swab specimens was extracted using one of the three platforms: the easyMAG (BioMerieux, Quebec, Canada), the KingFisher Flex automated extraction and purification systems (Thermo Fisher), or the Hamilton STARlet automated extractor (Hamilton, Reno, NV). The specimen input was 200 μL, and the purified nucleic acid was extracted into 100 μL total volume of the RNA extract from each specimen. An aliquot of 1−4 μL of RNA extract was used as the sample input for the one-tube RT-RPA-Cas12a assay of the S gene of SARS-CoV-2.

RESULTS AND DISCUSSION

Integration of Reverse Transcription (RT), Recombinase Polymerase Amplification (RPA), and CRISPR-Cas12a Detection in a Single Tube. The overall process of integrating reverse transcription (RT), recombinase polymerase amplification (RPA), and CRISPR-Cas12a-mediated signal generation, in order to detect a specific RNA in a single tube under isothermal conditions (40 °C), is shown in Figure 1. We use the detection of the viral RNA of SARS-CoV-2 as an example to illustrate the principles of our integrated RT-RPA-CRISPR-Cas12a assay, which includes the following reactions in one tube: reverse transcription of the RNA template producing a complementary DNA (cDNA), removal of the RNA template from cDNA by RNase H, exponential amplification of the cDNA by RPA, CRISPR RNA (crRNA)-directed recognition of dsDNA amplicons by the crRNA-Cas12a ribonucleoprotein (RNP), and multiple cleavage of quencher-fluorophore ssDNA reporters by the activated RNP, resulting in detectable fluorescence.

Optimization of RPA-CRISPR-Cas12a in a Single Tube. To integrate RPA with CRISPR-Cas12a detection for high sensitivity and specificity, we first examined the detection of a specific DNA sequence, which was reverse transcribed from a conserved region of SARS-CoV-2 RNA within the spike (S)

https://doi.org/10.1021/acs.analchem.1c03456
Anal. Chem. 2021, 93, 12808−12816

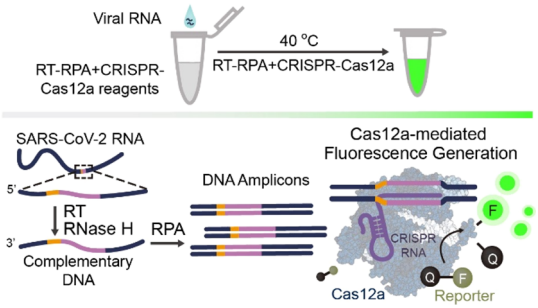


Figure 1. Schematics showing integration of reverse transcription (RT), recombinase polymerase amplification (RPA), and CRISPR-Cas12a-mediated fluorescence generation for isothermal (40 °C) single-tube detection of specific RNA. Once a sample is added to a reaction tube containing RT-RPA and CRISPR-Cas12a reagents, the tube is kept closed and maintained at 40 °C. RPA primers and reverse transcriptase interact with the target RNA to produce a complementary DNA (cDNA). RNase H cleaves the RNA template to make the cDNA free for exponential amplification by RPA. Directed by the CRISPR RNA (crRNA), the crRNA-Cas12a ribonucleoprotein (RNP) recognizes and binds to the specific sequence (shown in orange and purple) in dsDNA amplicons. Sequence-specific binding of the RNP/dsDNA complex activates the *trans*-cleavage activity of Cas12a, resulting in cleavage of short ssDNA reporters and thereby generating fluorescence.

protein. We chose to target dsDNA using CRISPR-Cas12a because CRISPR-Cas12a has a higher specificity for dsDNA than for ssDNA.[8] We designed a crRNA to target a specific sequence of dsDNA between the sequences recognized by the two RPA primers[15] (Figure S1). The CRISPR-targeting site contained a PAM domain of TTTV and a recognition domain of 20 nt (Figure S1).

We optimized the reaction conditions for both RPA and CRISPR-Cas12a, with an emphasis on maximizing the amplification efficiency of RPA and thus the signal generation capability of CRISPR-Cas12a. A higher concentration of Mg^{2+} (21 mM) than that recommended for the RPA kit (14 mM) enhanced the hybridization between the primers and the DNA templates, thus improving amplification and detection (Figure S2A). The optimum crRNA-Cas12a RNP concentration of 30 nM provided the fastest kinetics of nuclease activity for the amplified fluorescence detection (Figure S2B). The design and use of a shorter ssDNA reporter than those used by others minimized background fluorescence.

The integration of RPA and CRISPR-Cas12a reactions in one tube resulted in the successful detection of the specific DNA sequences corresponding to the S gene of SARS-CoV-2. The overall reaction took only 5−22 min to detect DNA ranging from 10^6 copies to 5 copies (Figure 2). The intensity of the fluorescence signals increases with the concentration of the target DNA. We determined that the measured fluorescence intensity of 150,000 (arbitrary unit) or higher corresponded to the visible fluorescence easily recognizable by the naked eyes (Figure S3). The time needed to reach this threshold fluorescence intensity was correlated inversely with the concentration of the target DNA (Figure 2B). The detection of five copies of DNA took only 22 min to reach the threshold fluorescence intensity of 150,000.

Challenges and Necessity for Rapid Initiation of the RPA Reaction. Having succeeded in rapid and sensitive detection of DNA, we extended the assay to the detection of viral RNA from SARS-CoV-2. The assay was able to detect high concentrations of RNA. However, the detection of 10,000 copies of RNA required 35 min (Figure S4), whereas the detection of only five copies of the equivalent DNA sequence was achieved in 22 min (Figure 2B). We investigated this dramatic decrease in sensitivity for the detection of RNA compared to the detection of DNA. We hypothesized that reverse transcription of RNA to cDNA delayed the initiation of the RPA reaction. We reasoned that the slow initiation of RPA could cause two problems in the one-tube assay: (1) nonspecific amplification reactions could consume the RPA reagents, and (2) the activity of the crRNA-Cas12 RNP decreased over time prior to its activation by the target dsDNA amplicons.

We first examined nonspecific amplification products using SYBR Green detection. In the absence of the target, SYBR Green fluorescence was detectable within 10 min of the one-tube reactions (Figure S5). Although the nonspecific amplicons were not detectable by CRISPR-Cas12a, the nonspecific reactions could deplete RPA reagents and impede the detection of low copy numbers of the target RNA.

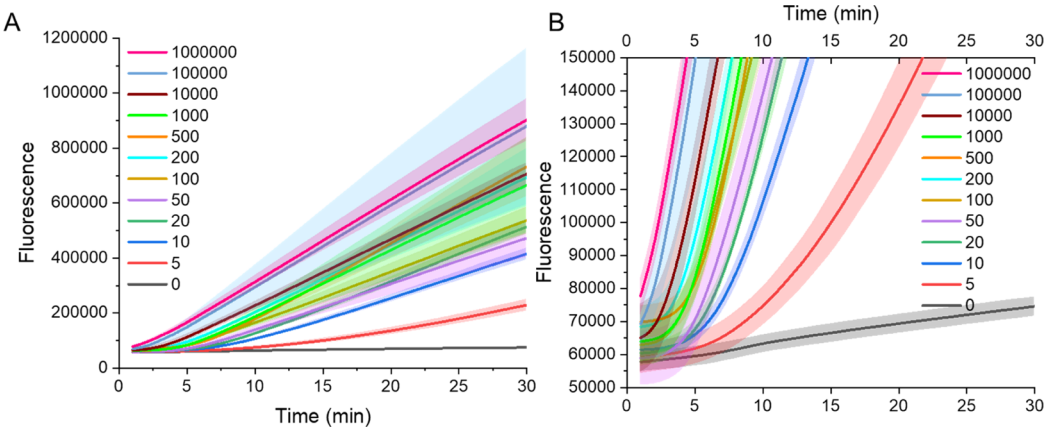


Figure 2. Fluorescence intensity, measured over time, from the single-tube RPA-Cas12a assay for the detection of the DNA sequence of the SARS-CoV-2 S gene, ranging from 5 copies to 10^6 copies. The standard deviation from triplicate analyses of each DNA concentration is shown as a matching colored band around each curve. (A) Fluorescence intensity measured over time. (B) Fluorescence intensity up to a set threshold value of 150,000 (arbitrary unit) and the time took to reach this threshold fluorescence intensity.

https://doi.org/10.1021/acs.analchem.1c03456
Anal. Chem. 2021, 93, 12808−12816

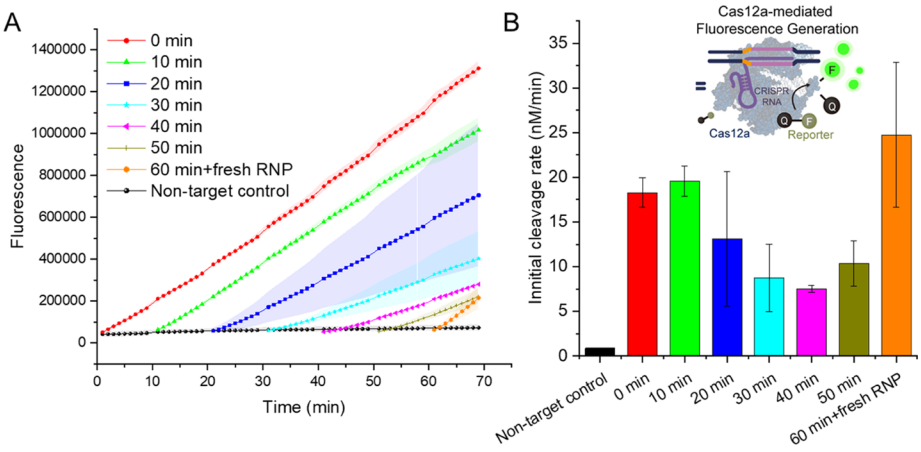


Figure 3. Stability of crRNA-Cas12a ribonucleoprotein (RNP) activity in the RPA reaction solution, measured by the fluorescence intensity of the reporter (A) and initial cleavage rate of the *trans*-cleavage activity of crRNA-Cas12a RNP (B). There was no amplification target in the mixture. Instead, a short dsDNA activator, containing only a CRISPR-targeting sequence but no primer binding sequence, was used to activate the RNP. The dsDNA activator (10 nM, 1.25 μL) and a quencher-fluorophore-labeled ssDNA reporter (100 μM, 1.25 μL) were added to separate tubes containing RPA reagents (11 μL) and RNP (0.5 μM, 1 μL) at different delay times (0−50 min). At a delay time of 60 min, fresh RNP (0.5 μM, 1 μL), along with the DNA activator and reporter, was added. The *trans*-cleavage of the quencher-fluorophore-labeled ssDNA reporter by the RNP generated fluorescence. The initial cleavage rate in Figure 3B was calculated by converting the slopes of curves in Figure 3A to the concentration of reporters cleaved in 1 min based on a calibration curve of fluorescence intensity *vs* concentration of reporters cleaved (Figure S6C).

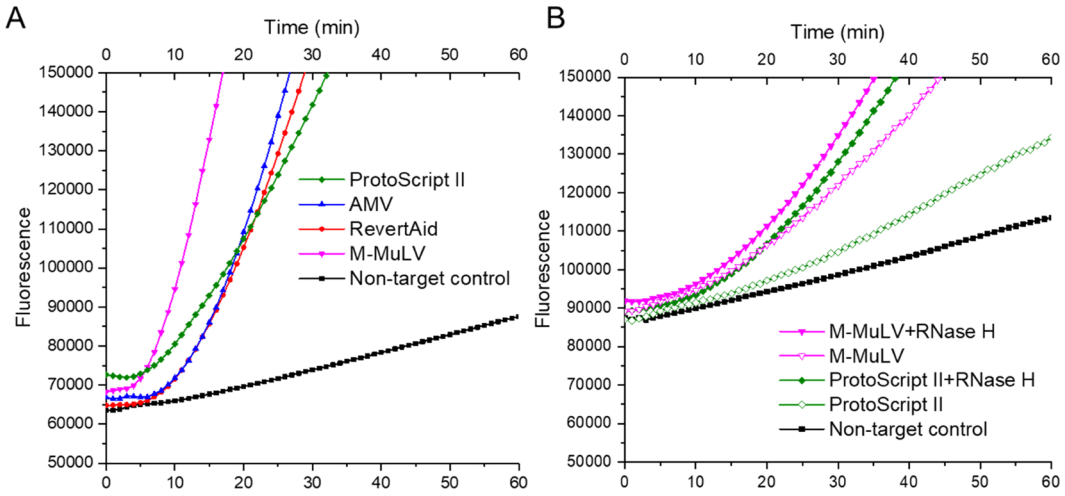


Figure 4. Comparison of reverse transcriptases and supplementation of RNase H in the detection of the S gene of SARS-CoV-2 RNA using the integrated RT-RPA-Cas12a assay. (A) Comparison of four reverse transcriptases used in the detection of 1000 copies of SARS-CoV-2 RNA, namely, ProtoScript II (200 U/μL, 0.5 μL/reaction), AMV (10 U/μL, 0.5 μL/reaction), RevertAid (200 U/μL, 0.5 μL/reaction), and M-MuLV (200 U/μL, 0.5 μL/reaction). (B) Addition of RNase H to the RT-RPA-Cas12a reaction mixture for the detection of 100 copies of SARS-CoV-2 RNA.

To understand the second problem, we tested the activity of the crRNA-Cas12a RNP in a scenario in which the DNA required to activate the RNP (DNA activator) was added after a time of delay. Normally, when the RNP was activated without delay (red curve in Figure 3A and Figure S6A), its catalytic activity remained over time (70 min) as indicated by the continuing increase of fluorescence due to the *trans*-cleavage of the reporters by the RNP. However, when the addition of the DNA activator was delayed by 20−50 min, the slower increase of fluorescence over time indicated lower activity of the RNP. If the activation of RNP was delayed by 20 min in the reaction mixture of RPA and CRISPR-Cas12a, the RNP lost 30% of its activity as indicated by the reduced initial cleavage rate (Figure 3B). A 40 min delay of the RNP activation resulted in more than 50% loss of the RNP activity in the reaction mixture. The decrease in the activity of non-activated Cas12a RNP was not caused by changes in the buffer pH or concentration of reagents. When fresh RNP and DNA activator were added to the RPA reaction mixture after a 60 min delay, a normal activity (and initial cleavage rate as shown in Figure 3B and Figure S6B) was observed. These results suggest that the timely activation of the RNP by the DNA target is critical for the *trans*-cleavage activity of the RNP.

In the presence of all the reagents for RT, RPA, and CRISPR-Cas12a reactions in a single tube, both nonspecific amplification and loss of RNP activity occurred. Overcoming both problems requires the rapid generation of DNA amplicons from trace amounts of the RNA target and rapid initiation of RPA.

Removal of the RNA Template after Reverse Transcription Significantly Improves the Performance of the Single-Tube RT-RPA-Cas12a Assay. Reverse transcription

https://doi.org/10.1021/acs.analchem.1c03456
Anal. Chem. 2021, 93, 12808−12816

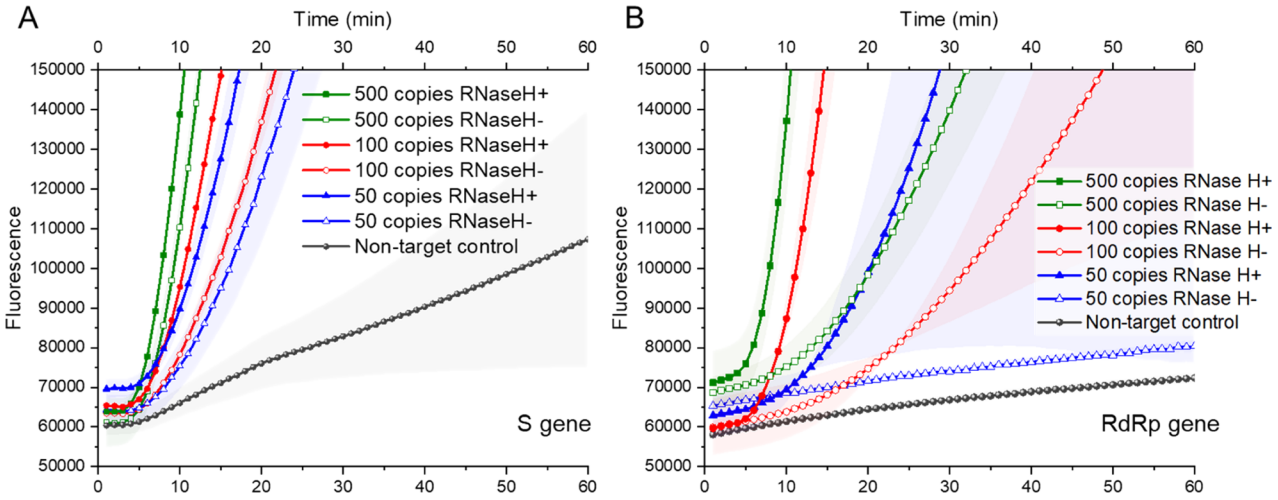


Figure 5. RNase H shortens the time for the positive detection of the RNA targets in both the S gene and RdRp gene. (A) Effect of RNase H treatment on the detection of the S gene cDNA at different concentrations. The RNA target (5×10^4 copies) was first reverse transcribed using ProtoScript II (NEB, M0368L) at 42 °C for 50 min in 1× ProtoScript II buffer with 1 μM of each RPA primer, 0.01 M DTT, and dNTP mix (1 mM each). Equal aliquots of the reverse transcription products were either treated with RNase H (1 U for 5 μL cDNA) at 42 °C for 10 min or an equivalent amount of water. The enzymes were then inactivated at 80 °C for 5 min. Serial dilutions corresponding to cDNA concentrations of 50, 100, and 500 copies/reaction were made and analyzed using the RPA-Cas12a assay. (B) Effect of RNase H treatment on the detection of the RdRp gene cDNA at different concentrations. Experimental procedures were the same as for the detection of the S gene, except RPA primers RdRP-F2-5 and Rd-R1, and CRISPR RNA RdRp-crRNA3 were used (sequences in Figure S8).

of RNA and dissociation of the RNA-cDNA hybrid are two potential critical processes leading to rapid RPA initiation. We compared four different reverse transcriptases, Protoscript II,[28] AMV,[29] RevertAid,[30] and M-MuLV,[31] used in our assay for the detection of SARS-CoV-2 RNA (Figure 4). With M-MuLV, the assay required only 15 min to produce a fluorescence intensity of 150,000 (arbitrary unit), whereas 30 min was needed when the other three reverse transcriptases were used (Figure 4A). M-MuLV is known to have a "functional RNase H domain", whereas the other three reverse transcriptases have either reduced or no RNase H activities.[28−31] The endoribonuclease activity of RNase H catalyzes the hydrolysis of phosphodiester bonds of RNA in RNA-DNA hybrids.[32] The removal of RNA from the RNA-cDNA hybrids leaves cDNA free to hybridize with RPA primers for amplification. We hypothesized that RNase H and its ability to remove RNA from the cDNA played an important role in fast RPA initiation.

To test the requirement for RNase H, we conducted assays with or without supplementing the single-tube mixtures of RT, RPA, and CRISPR-Cas12a reactions with RNase H (Figure 4B). One hundred copies of SARS-CoV-2 RNA were detectable in 44 min using the M-MuLV reverse transcriptase, which has a functional RNase domain. Supplementing the reaction with additional RNase H resulted in a shorter time (35 min) to produce equivalent fluorescence for the detection of the same amount of RNA. When Protoscript II was used as the reverse transcriptase, the assay could not yield a positive detection of 100 copies of SARS-CoV-2 RNA after 60 min. With the addition of RNase H to the reaction mixture, the detection of this low number of RNA molecules was achieved in 38 min (Figure 4B). These results demonstrate the importance of including RNase H to the single-tube reaction mixture. The addition of RNase H did not impair the *trans*-cleavage activity of Cas12a (Figure S7).

To further confirm that the treatment of the RNA-cDNA hybrid with RNase H was important for the detection of low copy numbers of SARS-CoV-2 RNA, we separated the reverse transcription of viral RNA from the subsequent RPA-Cas12a reaction and prepared RNA-cDNA hybrids using ProtoScript II. Since ProtoScript II reverse transcriptase has little RNase H activity, and the reaction temperature is relatively low (37−40 °C), RNA-cDNA hybrids remain after reverse transcription. We then left half aliquot untreated as RNA-cDNA hybrids and added RNase H to the other aliquot to obtain free cDNA. Both aliquots were subsequently inactivated, diluted, and analyzed using the RPA-Cas12a assay. RNase H treatment shortened the time to the positive detection of various amounts of RNA ranging from 50 to 500 copies per reaction (Figure 5A). The enhancement by the addition of RNase H was more significant at lower concentrations of the target RNA. We confirmed the finding of the RNase H treatment by extending the approach to the detection of low copy numbers of the RdRp gene of SARS-CoV-2 (Figure 5B and Figure S8). Fifty copies of the RdRp gene were detectable only after RNase H was added to the reaction (Figure 5B).

Our result demonstrated the necessity of RNase H in the single-tube assay of viral RNA involving RT, RPA, and CRISPR-12a reactions. The observed differences in the overall sensitivity between DNA detection and RNA detection may be explained by the requirement for rapid initiation of RPA and the function of the main proteins involved in RPA. For the detection of DNA by RPA, the interaction of primers with the template is facilitated by a recombinase and an ssDNA-binding protein (SSB). The recombinase unwinds dsDNA and allows the primers to hybridize with the template strand for the subsequent polymerase extension. SSB binds to the displaced strand, preventing the primers from being displaced.[11] However, in RNA detection, the RNA-cDNA hybrid formed after the reverse transcription of RNA has a lower binding affinity to SSB. Without SSB to bind and hold onto the displaced RNA strand, the ability of RPA to load the primers to the template is decreased. Therefore, additional RNase H activity is required to remove RNA from RNA-cDNA hybrids, making cDNA available for the rapid initiation of RPA.

https://doi.org/10.1021/acs.analchem.1c03456
Anal. Chem. 2021, 93, 12808−12816

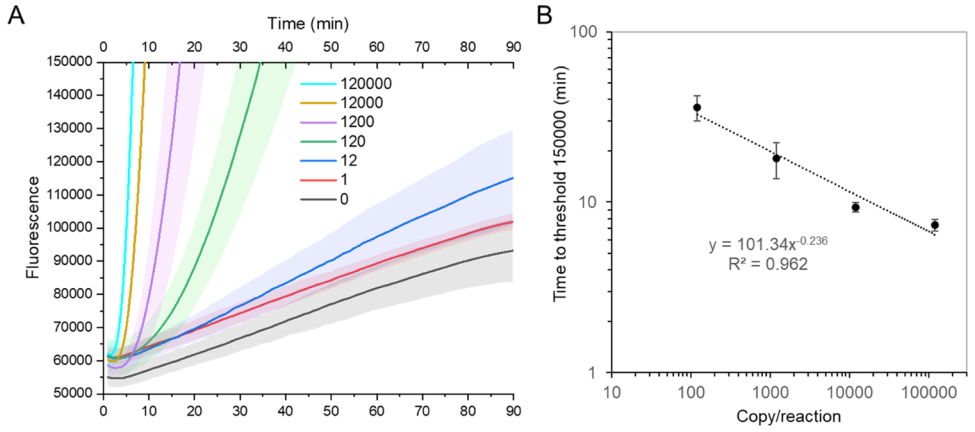


Figure 6. Detection of the S gene of SARS-CoV-2 RNA using the single-tube RT-RPA-Cas12a assay. (A) Fluorescence generation over time in response to the SARS-CoV-2 RNA extracted from the Vero E6 cell culture medium. The standard deviation of triplicates in each SARS-CoV-2 RNA concentration is shown as a shadow around the curve in the same hue. (B) Correlation of time to threshold and concentration of SARS-CoV-2 RNA.

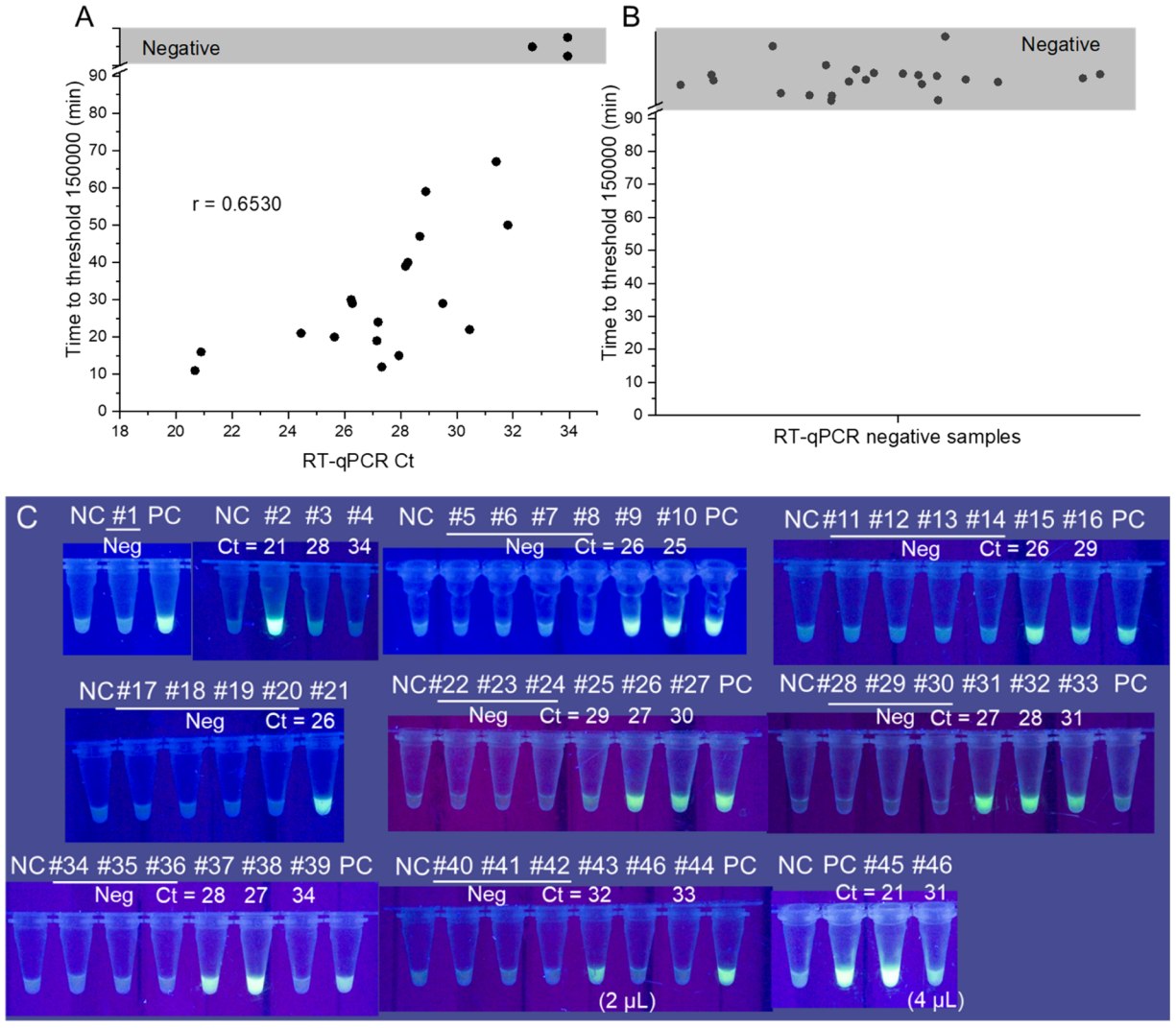


Figure 7. Results from the RT-RPA-Cas12a analysis of 46 clinical upper respiratory swab samples using real-time fluorescence detection (A, B) and end-point (90 min) visualization (C). (A) Correlation between the results of RT-RPA-Cas12a analysis and RT-qPCR analysis of 21 positive samples. The time to reach the threshold fluorescence of 150,000 (arbitrary unit) was obtained from continued real-time monitoring of fluorescence at 1 min intervals. (B) Results of RT-RPA-Cas12a analysis and RT-qPCR analysis of 25 negative samples. None of the negative samples reached threshold fluorescence after 90 min of reaction. (C) End-point fluorescence visualization of 46 samples along with negative controls (NC) and positive controls (PC).

https://doi.org/10.1021/acs.analchem.1c03456
Anal. Chem. 2021, 93, 12808−12816

Single-Tube RT-RPA-CRISPR-Cas12a Assay for the Detection of SARS-CoV-2 RNA. We successfully integrated RT, RPA, and CRISPR-Cas12a into a single tube for the detection of SARS-CoV-2 RNA. Compared with adding CRISPR-Cas12a at the end of RT-RPA reaction, real-time monitoring of the fluorescence signal in this single-tube assay also provided the relative SARS-CoV-2 RNA concentration (Figure S9). Viral RNA was extracted from a SARS-CoV-2-infected Vero-E6 cell culture medium and diluted to various concentrations, ranging from 10^5 copies/reaction to 1 copy/reaction. We were able to detect 120 copies of viral RNA in under 40 min (Figure 6A). However, we observed an increasing variation among repeat tests of viral RNA samples with low copy numbers. In two of the three tests of 12 copies of viral RNA per reaction, the fluorescence signals were increasing and could be differentiated from background; however, the fluorescence intensity did not reach the threshold value of 150,000 within 90 min. We therefore examined the reproducibility of our assay for the detection of low copy numbers of viral RNA. Viral RNA ranging from 50 to 400 copies was analyzed in nine replicate experiments. We consistently detected 9 positives in all 9 tests when 200 or more copies of viral RNA were present in each reaction (Figure S10). The detection of very low numbers of RNA was less consistent, resulting in 8 positives in 9 tests of 100 copies of SARS-CoV-2 RNA/reaction and 7 positives in 9 tests of 50 copies/reaction. The limit of detection for RNA, 200 copies/reaction (or 50 copies/μL of RNA extract sample), meets the sensitivity requirement for the population SARS-CoV-2 screening test, which is estimated to be 100 copies/μL.[33] The S gene target of SARS-CoV-2 is sufficiently different from the corresponding regions in SARS-CoV and MERS-CoV (Figure S11) for the CRIPSR-Cas12a RNP to differentiate them. Thus, the SARS-CoV and MERS-CoV gene (10^4 copies/reaction) did not generate any false positive result (Figure S11).

While other RPA-based assays have primarily been used for binary positive or negative screening tests, our RT-RPA-Cas12a assay provided a semi-quantitative detection of SARS-CoV-2 RNA in a range of 100 to 100,000 copies/reaction (Figure 6B). The time to threshold correlated with the concentrations of SARS-CoV-2 RNA in the samples. Detection of SARS-CoV-2 RNA at concentrations over 10^5 copies (Ct = 18) was achieved in 7 min with the RT-RPA-Cas12a assay (Figure 6B and Figure S12).

Analysis of RNA Extracted from Respiratory Swab Clinical Samples. We applied our single-tube assay to upper respiratory swab samples collected from 46 patients for COVID-19 diagnosis at Alberta Precision Laboratories (APL). APL analyzed RNA extracts by RT-qPCR for the E gene or the N gene and found that 25 samples were negative and 21 were positive with Ct values ranging from 19 to 34. We analyzed an aliquot (1−4 μL) of the sample extract using our single-tube RT-RPA-Cas12a assay. We successfully identified all the negative samples as negative (Figure 7B) and 18 of the positive samples as positive (Figure 7A). Three samples (#4, #39, and #44) that required 33.9, 33.9, and 32.7 cycles (Ct) to achieve positive detection using RT-qPCR did not reach the fluorescence intensity of 150,000 within 90 min using the RT-RPA-Cas12a assay. This was expected because the concentration of viral RNA was very low (<20 copies of S gene per reaction) in these three samples and the sample volume used for the RT-RPA-Cas12a assay (1−4 μL) was less than half for the RT-qPCR analysis (5−10 μL). Nonetheless, the results of the 18 positive samples from these two assays were consistent, with a Pearson correlation coefficient of 0.653 between the Ct values from RT-qPCR and the time to threshold from the RT-RPA-Cas12a analysis (Figure 7A).

We also visualized the end-point fluorescence of all the 46 samples using our RT-RPA-Cas12a assay, thereby avoiding the use of an expensive RT-qPCR instrument. We were able to differentiate the positive samples with bright fluorescence from the negative samples with almost no fluorescence (Figure 7C). The results were consistent with our real-time fluorescence detection (Figure 7A,B, Figure S13).

CONCLUSIONS

We integrated reverse transcription (RT), recombinase polymerase amplification (RPA), and Cas12a-mediated detection in a single tube for rapid and sensitive RNA detection. We first achieved the detection of a few copies of DNA in 20 min using the integrated RPA-Cas12a assay, but our initial attempt showed that the assay did not perform as well for RNA detection. Our study on the compatibility of RT, RPA, and Cas12a-mediated detection suggested the importance of rapid reverse transcription reaction and RPA initiation because once all the reagents are mixed in a single tube, both nonspecific RPA amplification and loss of Cas12a RNP activity occur.

We identified the importance of RNase H on the overall reaction rate and sensitivity of the RT-RPA-Cas12a assay in a single tube for the detection of RNA. Free cDNA initiates the RPA-Cas12a reaction more efficiently than RNA-cDNA hybrids. When the RNA copy number is very low, there is little freely available cDNA. RNase H removed the RNA from RNA-cDNA hybrids and significantly enhanced the performance of the integrated RT-RPA-Cas12a assay. Research focusing on the development of RT-RPA techniques has also reported the importance of RNase H by quantifying the RPA products at the end of the reaction with qPCR.[34] The real-time monitoring of our assay provides information on how the choice of reverse transcription and the addition of RNase H affect the reaction kinetics.

With RNase H and the carefully optimized formulation of our one-tube RT-RPA-Cas12a assay, we are able to amplify and detect over 200 copies of S gene per reaction within 5−30 min incubation. Our results from the analysis of respiratory swab clinical samples using real-time fluorescence monitoring of our assay are correlated with the concentration of SARS-CoV-2 RNA quantified by RT-qPCR. The CRISPR-based detection improves the assay specificity. Our assay operates at one temperature (40 °C) in a single tube and uses different reagents from those of RT-PCR, thus holding promise to complement current tests for COVID-19 screening. For point-of-care testing, the test results can be directly visualized under UV light or detected by a portable fluorescence reader for semi-quantitative readings.

ASSOCIATED CONTENT

Supporting Information

The Supporting Information is available free of charge at https://pubs.acs.org/doi/10.1021/acs.analchem.1c03456.

Additional experimental details, materials, and methods, including optimization results, performance compar-

https://doi.org/10.1021/acs.analchem.1c03456
Anal. Chem. 2021, 93, 12808−12816

isons, and sequences of primers, crRNA, and the targets (PDF)

AUTHOR INFORMATION

Corresponding Authors

Hongquan Zhang − *Division of Analytical and Environmental Toxicology, Department of Laboratory Medicine and Pathology, Faculty of Medicine and Dentistry, University of Alberta, Edmonton, Alberta T6G 2G3, Canada;* orcid.org/0000-0003-1088-9862; Email: hongquan@ualberta.ca

X. Chris Le − *Division of Analytical and Environmental Toxicology, Department of Laboratory Medicine and Pathology, Faculty of Medicine and Dentistry, University of Alberta, Edmonton, Alberta T6G 2G3, Canada;* orcid.org/0000-0002-7690-6701; Phone: 1-780-492-6416; Email: xc.le@ualberta.ca; Fax: 1-780-492-7800

Authors

Wei Feng − *Division of Analytical and Environmental Toxicology, Department of Laboratory Medicine and Pathology, Faculty of Medicine and Dentistry, University of Alberta, Edmonton, Alberta T6G 2G3, Canada;* orcid.org/0000-0003-1081-7914

Hanyong Peng − *Division of Analytical and Environmental Toxicology, Department of Laboratory Medicine and Pathology, Faculty of Medicine and Dentistry, University of Alberta, Edmonton, Alberta T6G 2G3, Canada; State Key Laboratory of Environmental Chemistry and Ecotoxicology, Research Center for Eco-Environmental Sciences, Chinese Academy of Sciences, Beijing 100085, China;* orcid.org/0000-0001-7079-0827

Jingyang Xu − *Division of Analytical and Environmental Toxicology, Department of Laboratory Medicine and Pathology, Faculty of Medicine and Dentistry, University of Alberta, Edmonton, Alberta T6G 2G3, Canada*

Yanming Liu − *Division of Analytical and Environmental Toxicology, Department of Laboratory Medicine and Pathology, Faculty of Medicine and Dentistry, University of Alberta, Edmonton, Alberta T6G 2G3, Canada*

Kanti Pabbaraju − *Provincial Laboratory for Public Health (ProvLab), Alberta Precision Laboratories, Calgary, Alberta T2N 4W4, Canada*

Graham Tipples − *Provincial Laboratory for Public Health, Alberta Precision Laboratories, University of Alberta Hospitals, Edmonton, Alberta T6G 2J2, Canada; Li Ka Shing Institute of Virology, Department of Medical Microbiology and Immunology, Faculty of Medicine and Dentistry, University of Alberta, Edmonton, Alberta T6G 2E1, Canada*

Michael A. Joyce − *Li Ka Shing Institute of Virology, Department of Medical Microbiology and Immunology, Faculty of Medicine and Dentistry, University of Alberta, Edmonton, Alberta T6G 2E1, Canada*

Holly A. Saffran − *Li Ka Shing Institute of Virology, Department of Medical Microbiology and Immunology, Faculty of Medicine and Dentistry, University of Alberta, Edmonton, Alberta T6G 2E1, Canada*

D. Lorne Tyrrell − *Li Ka Shing Institute of Virology, Department of Medical Microbiology and Immunology, Faculty of Medicine and Dentistry, University of Alberta, Edmonton, Alberta T6G 2E1, Canada*

Shawn Babiuk − *National Centre for Foreign Animal Disease, Canadian Food Inspection Agency, Winnipeg, Manitoba R3E 3M4, Canada*

Complete contact information is available at: https://pubs.acs.org/10.1021/acs.analchem.1c03456

Author Contributions

[▽]W.F. and H.P. contributed equally to this work.

Notes

The authors declare no competing financial interest.

ACKNOWLEDGMENTS

We thank the Canadian Institutes of Health Research, the New Frontiers in Research Fund, the Natural Sciences and Engineering Research Council of Canada, and Li Ka Shing Institute of Virology for their support. W.F. acknowledges the support of Graduate Scholarships from the China Scholarship Council and Alberta Innovates.

REFERENCES

(1) Jinek, M.; Chylinski, K.; Fonfara, I.; Hauer, M.; Doudna, J. A.; Charpentier, E. *Science* **2012**, *337*, 816−821.

(2) Cong, L.; Ran, F. A.; Cox, D.; Lin, S.; Barretto, R.; Habib, N.; Hsu, P. D.; Wu, X.; Jiang, W.; Marraffini, L. A.; Zhang, F. *Science* **2013**, *339*, 819−823.

(3) Mali, P.; Yang, L.; Esvelt, K. M.; Aach, J.; Guell, M.; DiCarlo, J. E.; Norville, J. E.; Church, G. M. *Science* **2013**, *339*, 823−826.

(4) East-Seletsky, A.; O'Connell, M. R.; Knight, S. C.; Burstein, D.; Cate, J. H. D.; Tjian, R.; Doudna, J. A. *Nature* **2016**, *538*, 270−273.

(5) Gootenberg, J. S.; Abudayyeh, O. O.; Lee, J. W.; Essletzbichler, P.; Dy, A. J.; Joung, J.; Verdine, V.; Donghia, N.; Daringer, N. M.; Freije, C. A.; Myhrvold, C.; Bhattacharyya, R. P.; Livny, J.; Regev, A.; Koonin, E. V.; Hung, D. T.; Sabeti, P. C.; Collins, J. J.; Zhang, F. *Science* **2017**, *356*, 438−442.

(6) Knott, G. J.; Doudna, J. A. *Science* **2018**, *361*, 866−869.

(7) Gaj, T.; Gersbach, C. A.; Barbas, C. F., III *Trends Biotechnol.* **2013**, *31*, 397−405.

(8) Chen, J. S.; Ma, E.; Harrington, L. B.; Da Costa, M.; Tian, X.; Palefsky, J. M.; Doudna, J. A. *Science* **2018**, *360*, 436−439.

(9) Harrington, L. B.; Burstein, D.; Chen, J. S.; Paez-Espino, D.; Ma, E.; Witte, I. P.; Cofsky, J. C.; Kyrpides, N. C.; Banfield, J. F.; Doudna, J. A. *Science* **2018**, *362*, 839−842.

(10) Notomi, T.; Okayama, H.; Masubuchi, H.; Yonekawa, T.; Watanabe, K.; Amino, N.; Hase, T. *Nucleic Acids Res.* **2000**, *28*, E63.

(11) Piepenburg, O.; Williams, C. H.; Stemple, D. L.; Armes, N. A. *PLoS Biol.* **2006**, *4*, No. e204.

(12) Myhrvold, C.; Freije, C. A.; Gootenberg, J. S.; Abudayyeh, O. O.; Metsky, H. C.; Durbin, A. F.; Kellner, M. J.; Tan, A. L.; Paul, L. M.; Parham, L. A.; Garcia, K. F.; Barnes, K. G.; Chak, B.; Mondini, A.; Nogueira, M. L.; Isern, S.; Michael, S. F.; Lorenzana, I.; Yozwiak, N. L.; MacInnis, B. L.; Bosch, I.; Gehrke, L.; Zhang, F.; Sabeti, P. C. *Science* **2018**, *360*, 444−448.

(13) Joung, J.; Ladha, A.; Saito, M.; Kim, N.-G.; Woolley, A. E.; Segel, M.; Barretto, R. P. J.; Ranu, A.; Macrae, R. K.; Faure, G.; Ioannidi, E. I.; Krajeski, R. N.; Bruneau, R.; Huang, M.-L. W.; Yu, X. G.; Li, J. Z.; Walker, B. D.; Hung, D. T.; Greninger, A. L.; Jerome, K. R.; Gootenberg, J. S.; Abudayyeh, O. O.; Zhang, F. *New Engl. J. Med.* **2020**, *383*, 1492−1494.

(14) Broughton, J. P.; Deng, X.; Yu, G.; Fasching, C. L.; Servellita, V.; Singh, J.; Miao, X.; Streithorst, J. A.; Granados, A.; Sotomayor-Gonzalez, A.; Zorn, K.; Gopez, A.; Hsu, E.; Gu, W.; Miller, S.; Pan, C.-Y.; Guevara, H.; Wadford, D. A.; Chen, J. S.; Chiu, C. Y. *Nat. Biotechnol.* **2020**, *38*, 870−874.

(15) Zhang, F.; Abudayyeh, O. O.; Gootenberg, J. S. *A protocol for detection of COVID-19 using CRISPR diagnostics 2020.* https://www.

broadinstitute.org/files/publications/special/COVID-19%20detection%20(updated).pdf.
(16) Wu, K. J. *These researchers tested positive. But the virus wasn't the cause. Several scientists working with harmless genetic material have discovered that their research may have contaminated their coronavirus tests. New York Times November 12, 2020.* https://www.nytimes.com/2020/11/12/health/coronavirus-testing-lab-contamination.html (accessed May 2, 2021).
(17) New England BioLabs *EnGen® Lba Cas12a (Cpf1)*. https://www.neb.ca/detail.php?id=m0653 (accessed May 2, 2021).
(18) Yin, K.; Ding, X.; Li, Z.; Zhao, H.; Cooper, K.; Liu, C. *Anal. Chem.* **2020**, *92*, 8561−8568.
(19) Kellner, M. J.; Koob, J. G.; Gootenberg, J. S.; Abudayyeh, O. O.; Zhang, F. *Nat. Protoc.* **2019**, *14*, 2986−3012.
(20) Guo, L.; Sun, X.; Wang, X.; Liang, C.; Jiang, H.; Gao, Q.; Dai, M.; Qu, B.; Fang, S.; Mao, Y.; Chen, Y.; Feng, G.; Gu, Q.; Wang, R. R.; Zhou, Q.; Li, W. *Cell Discovery* **2020**, *6*, 34.
(21) Sun, Y.; Yu, L.; Liu, C.; Ye, S.; Chen, W.; Li, D.; Huang, W. *J. Transl. Med.* **2021**, *19*, 74.
(22) Wang, Y.; Ke, Y.; Liu, W.; Sun, Y.; Ding, X. *ACS Sens.* **2020**, *5*, 1427−1435.
(23) Ding, X.; Yin, K.; Li, Z.; Lalla, R. V.; Ballesteros, E.; Sfeir, M. M.; Liu, C. *Nat. Commun.* **2020**, *11*, 4711.
(24) Arizti-Sanz, J.; Freije, C. A.; Stanton, A. C.; Petros, B. A.; Boehm, C. K.; Siddiqui, S.; Shaw, B. M.; Adams, G.; Kosoko-Thoroddsen, T.-S. F.; Kemball, M. E.; Uwanibe, J. N.; Ajogbasile, F. V.; Eromon, P. E.; Gross, R.; Wronka, L.; Caviness, K.; Hensley, L. E.; Bergman, N. H.; MacInnis, B. L.; Happi, C. T.; Lemieux, J. E.; Sabeti, P. C.; Myhrvold, C. *Nat. Commun.* **2020**, *11*, 5921.
(25) Ding, X.; Yin, K.; Li, Z.; Liu, C. All-in-One Dual CRISPR-Cas12a (AIOD-CRISPR) assay: A case for rapid, ultrasensitive and visual detection of novel coronavirus SARS-CoV-2 and HIV virus. *BioRxiv* 2020, DOI: 10.1101/2020.03.19.998724.
(26) de Puig, H.; Lee, R. A.; Najjar, D.; Tan, X.; Soekensen, L. R.; Angenent-Mari, N. M.; Donghia, N. M.; Weckman, N. E.; Ory, A.; Ng, C. F.; Nguyen, P. Q.; Mao, A. S.; Ferrante, T. C.; Lansberry, G.; Sallum, H.; Niemi, J.; Collins, J. J. *Sci. Adv.* **2021**, *7*, eabh2944.
(27) Pabbaraju, K.; Wong, A. A.; Douesnard, M.; Ma, R.; Gill, K.; Dieu, P.; Fonseca, K.; Zelyas, N.; Tipples, G. A. *Off. J. Assoc. Med. Microbiol. Infect. Dis.* **2021**, *6*, 16−22.
(28) New England BioLabs *ProtoScript® II reverse transcriptase*. https://www.neb.ca/detail.php?id=m0368 (accessed May 2).
(29) New England BioLabs *AMV reverse transcriptase*. https://www.neb.ca/detail.php?id=m0277 (accessed May 2).
(30) Thermofisher *RevertAid reverse transcriptase*. https://www.thermofisher.com/order/catalog/product/EP0441#/EP0441 (accessed May 2).
(31) New England Biolabs *M-MuLV reverse transcriptase*. https://www.neb.ca/detail.php?id=m0368 (accessed May 2).
(32) Our Cell Biology Correspondent. *Nature* **1973**, *241*, 429−429.
(33) Larremore, D. B.; Wilder, B.; Lester, E.; Shehata, S.; Burke, J. M.; Hay, J. A.; Tambe, M.; Mina, M. J.; Parker, R. *Sci. Adv.* **2021**, *7*, eabd5393.
(34) Qian, J.; Boswell, S. A.; Chidley, C.; Lu, Z.-x.; Pettit, M. E.; Gaudio, B. L.; Fajnzylber, J. M.; Ingram, R. T.; Ward, R. H.; Li, J. Z.; Springer, M. *Nat. Commun.* **2020**, *11*, 5920.

https://doi.org/10.1021/acs.analchem.1c03456
Anal. Chem. 2021, 93, 12808−12816